Wei-Wen Yu International Specialty Conference on Cold-Formed Steel Structures
Baltimore, Maryland, U.S.A., November 9 & 10, 2016

Lateral-Torsional Buckling of General Cold-Formed Steel Beams

Robert S. Glauz, P.E.[1]

Abstract

The design of unbraced cold-formed steel beams must consider lateral-torsional buckling due to the low torsional stiffness associated with open cross-sections. The American Iron and Steel Institute incorporated design equations for the critical elastic lateral-torsional buckling stress in the North American Specification for the Design of Cold-Formed Steel Members. These equations are based on elastic theory for singly-symmetric and doubly-symmetric sections. However, the equation for point-symmetric sections is only a rough approximation. Furthermore, there are no provisions for lateral-torsional buckling of non-symmetric sections, or sections oriented to non-principal axes. This paper investigates and develops a general formulation of the lateral-torsional buckling equation to broadly cover all cold-formed steel cross-sections.

Introduction

Point-symmetric Zee sections are commonly used for structural members such as purlins, but the support directions do not typically align to the principal axes. The critical elastic lateral-torsional buckling stress is therefore more difficult to determine. The current AISI Specification provision for lateral-torsional buckling of point-symmetric sections is based on lateral-torsional buckling of a doubly-symmetric shape, with a reduction factor of 0.5 to roughly approximate its behavior. Numerical analysis has shown that this reduction factor can actually vary from 0.3 to 1.0 depending on section geometry.

It has also become more common in practice to use custom shapes as structural beams. This is often driven by application constraints, material optimization, and ease of material handling, among other factors. The current AISI Specification has no provisions for predicting the lateral-torsional buckling strength of non-symmetric sections, or beams where the support directions do not align with the principal axes.

---

[1] President/Owner, RSG Software, Inc., Lee’s Summit, Missouri, USA

The lateral-torsional buckling equations used today for symmetrical shapes were originally investigated by Vlasov (1961) and Timoshenko (1961), and further studied by Peköz (1969). This paper expands on these developments to consider the more general case of any cold-formed steel cross-section at any orientation. Numerous symbols are used in this investigation which are defined at the end of this paper.

Lateral-Torsional Buckling

An unbraced member subject to a sufficient bending moment may exhibit global buckling where the compression portion of the member translates laterally and rotates. Considering such a member oriented to its principal axes u and v, with compression and bending applied to the ends of the member, the differential equations of equilibrium are given in Eq. 1, adapted from Vlasov (1961) and Peköz (1969).

$$EI_v u'''' + Pu'' + P(v_o - e_v)\phi'' = 0 \tag{1}$$
$$EI_u v'''' + Pv'' - P(u_o - e_u)\phi'' = 0$$
$$EC_w\phi'''' - (GJ - 2\beta_v Pe_v - 2\beta_u Pe_u - Pr_o^2)\phi'' + P(v_o - e_v)u'' - P(u_o - e_u)v'' = 0$$

where the end moments are the product of the axial force P and its biaxial eccentricities ($M_u = Pe_v$, $M_v = Pe_u$), and the following geometric properties of the cross-section are defined:

$$\beta_v = \frac{U_u}{2I_u} - v_o \qquad \beta_u = \frac{U_v}{2I_v} - u_o \tag{2}$$

$$U_u = \int v^3 dA + \int u^2 v dA \qquad U_v = \int u^3 dA + \int v^2 u dA \tag{3}$$

$$I_u = \int v^2 dA \qquad I_v = \int u^2 dA \tag{4}$$

To solve these differential equations, the displacements u, v, and ϕ are assigned sinusoidal forms, which produce the following set of equations:

$$(P_v - P)A_1 + (Pe_v - Pv_o)A_3 = 0 \tag{5}$$
$$(P_u - P)A_2 - (Pe_u - Pu_o)A_3 = 0$$
$$(Pe_v - Pv_o)A_1 - (Pe_u - Pu_o)A_2 + [(P_t - P)r_o^2 - 2\beta_v Pe_v - 2\beta_u Pe_u]A_3 = 0$$

where

$$P_u = \pi^2 EI_u/L^2 \qquad P_v = \pi^2 EI_v/L^2 \qquad P_t = \frac{1}{r_o^2}(GJ + \pi^2 EC_w/L^2) \tag{6}$$

The solution to these simultaneous equations is obtained by equating the determinant of the coefficients on A_1, A_2, and A_3 to zero:

$$\begin{vmatrix} P_v - P & 0 & Pe_v - Pv_o \\ 0 & P_u - P & -Pe_u + Pu_o \\ Pe_v - Pv_o & -Pe_u + Pu_o & (P_t - P)r_o^2 - 2\beta_v Pe_v - 2\beta_u Pe_u \end{vmatrix} = 0 \qquad (7)$$

Expansion of this determinant gives the principal axis form of the flexural-torsional buckling equation for a member subjected to eccentric axial load:

$$\begin{gathered} (P_v - P)(P_u - P)[(P_t - P)r_o^2 - 2\beta_v Pe_v - 2\beta_u Pe_u] \\ -(P_u - P)(Pe_v - Pv_o)^2 - (P_v - P)(Pe_u - Pu_o)^2 = 0 \end{gathered} \qquad (8)$$

The development of a general form for non-principal axes would require a redevelopment of the differential equations of equilibrium to account for unsymmetric bending stress distributions in all three equations. This raises a number of complications which make it a difficult and undesirable approach.

This investigation pursues the problem by adapting the principal axis solution to a rotated coordinate system. Figure 1 shows an arbitrary cross-section with centroid *C* and shear center *O*, oriented to orthogonal centroidal *x* and *y* axes which represent the directions of the supports. The principal *u* and *v* axes are oriented at an angle α measured counterclockwise from the *x* and *y* axes, respectively.

If the axial force *P* is applied at point *E* on the *y* axis, the moment produced about the *x* axis is $M_x = Pe_y$. The eccentricities associated with point *E* relative to the principal axes are given by e_u and e_v as follows:

$$e_u = e_y \sin\alpha \qquad\qquad e_v = e_y \cos\alpha \qquad (9)$$

The application of a pure moment M_x is achieved by increasing the eccentricity e_y while decreasing the axial load *P*. Substituting the expressions in Eq. 9 into Eq. 8, and taking the limit as e_y approaches infinity and *P* approaches zero produces the following equation in terms of M_x:

$$\begin{gathered} P_u P_v P_t r_o^2 - 2\beta_v P_u P_v M_x \cos\alpha - 2\beta_u P_u P_v M_x \sin\alpha \\ -P_u M_x^2 \cos^2\alpha - P_v M_x^2 \sin^2\alpha = 0 \end{gathered} \qquad (10)$$

This is rearranged into quadratic form as Eq. 11. It is then convenient to assign the nomenclature P'_y and β_y as defined in Eq. 12 to simplify the lateral-torsional buckling solution to Eq. 13.

$$\frac{P_u \cos^2 \alpha + P_v \sin^2 \alpha}{P_u P_v} M_x^2 + 2(\beta_v \cos \alpha + \beta_u \sin \alpha) M_x - P_t r_o^2 = 0 \tag{11}$$

$$P'_y = \frac{P_u P_v}{P_u \cos^2 \alpha + P_v \sin^2 \alpha} \qquad \beta_y = \beta_v \cos \alpha + \beta_u \sin \alpha \tag{12}$$

$$\boxed{M_x = P'_y \left[-\beta_y \pm \sqrt{\beta_y^2 + r_o^2 P_t / P'_y} \right]} \tag{13}$$

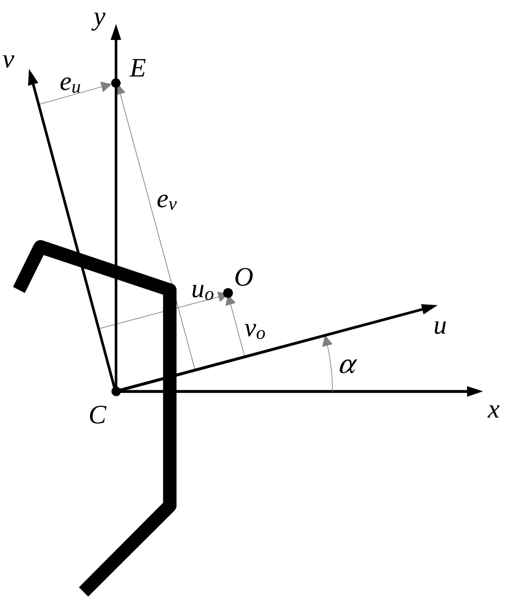

Figure 1. Arbitrary cross-section oriented to x and y support directions

The same approach can be used for developing the lateral-torsional buckling moment about the *y* axis. If point *E* is placed on the *x* axis, producing moment $M_y = Pe_x$, the following eccentricity relationships exist:

$$e_u = e_x \cos \alpha \qquad e_v = -e_x \sin \alpha \tag{14}$$

Substituting the expressions in Eq. 14 into Eq. 8, and taking the limit as e_x approaches infinity and *P* approaches zero produces Eq. 15 in terms of M_y, with the quadratic form shown as Eq. 16. Then assigning the nomenclature for P'_x and β_x as defined in Eq. 17 simplifies the M_y lateral-torsional buckling solution to Eq. 18.

$$P_u P_v P_t r_o^2 + 2\beta_v P_u P_v M_y \sin\alpha - 2\beta_u P_u P_v M_y \cos\alpha$$
$$-P_u M_y^2 \sin^2\alpha - P_v M_y^2 \cos^2\alpha = 0 \tag{15}$$

$$\frac{P_v \cos^2\alpha + P_u \sin^2\alpha}{P_u P_v} M_y^2 + 2(\beta_u \cos\alpha - \beta_v \sin\alpha) M_x - P_t r_o^2 = 0 \tag{16}$$

$$P'_x = \frac{P_u P_v}{P_v \cos^2\alpha + P_u \sin^2\alpha} \qquad \beta_x = \beta_u \cos\alpha - \beta_v \sin\alpha \tag{17}$$

$$\boxed{M_y = P'_x\left[-\beta_x \pm \sqrt{\beta_x^2 + r_o^2 P_t / P'_x}\right]} \tag{18}$$

Axis Transformation

The expressions for P' and β in equations 12 and 17 use principal axis properties I_u, I_v, β_u, β_v, U_u, and U_v. Standard design procedures require section property calculations using the *x* and *y* axes which correspond to the member orientation. Numerical integration for both orientations requires additional effort, so the transformation of these properties between coordinate axes is beneficial.

The definitions for P'_y and P'_x in equations 12 and 17 can be factored as shown in Eq. 19. The principal axis moments of inertia must then be stated in terms of *x* and *y* axes.

$$P'_y = \frac{\pi^2 E}{L^2} \frac{I_u I_v}{I_u \cos^2\alpha + I_v \sin^2\alpha} \qquad P'_x = \frac{\pi^2 E}{L^2} \frac{I_u I_v}{I_v \cos^2\alpha + I_u \sin^2\alpha} \tag{19}$$

The location of each point in the cross-section is expressed in principal axis coordinates with the following relationships:

$$u = x\cos\alpha + y\sin\alpha \qquad v = y\cos\alpha - x\sin\alpha \tag{20}$$

Substituting Eq. 20 into the expressions for principal axis moments of inertia defined in Eq. 4 produces the following equations, where I_x and I_y are the moments of inertia about the *x* and *y* axes, and I_{xy} is the product of inertia.

$$I_u = I_x \cos^2\alpha + I_y \sin^2\alpha - 2I_{xy} \sin\alpha\cos\alpha \tag{21}$$
$$I_v = I_y \cos^2\alpha + I_x \sin^2\alpha + 2I_{xy} \sin\alpha\cos\alpha \tag{22}$$

From fundamental mechanics of materials, we recognize the following additional relationships derived using double-angle trigonometric identities and Mohr's circle:

$$\tan 2\alpha = \frac{-2I_{xy}}{I_x - I_y} \tag{23}$$

$$I_u\,,\ I_v = \frac{1}{2}\left(I_x + I_y\right) \pm \frac{1}{2}\sqrt{(I_x - I_y)^2 + 4I_{xy}^2} \tag{24}$$

$$I_u I_v = I_x I_y - I_{xy}^2 \tag{25}$$

$$I_x = I_u\,cos^2\,\alpha + I_v\,sin^2\,\alpha \qquad\qquad I_y = I_v\,cos^2\,\alpha + I_u\,sin^2\,\alpha \tag{26}$$

Substituting the relationships in Eq. 25 and Eq. 26 into Eq. 19 provides the definitions for P'_y and P'_x in terms of x and y section properties.

$$P'_y = P_y\left(1 - \frac{I_{xy}^2}{I_x I_y}\right) \qquad\qquad P'_x = P_x\left(1 - \frac{I_{xy}^2}{I_x I_y}\right) \tag{27}$$

where

$$P_y = \frac{\pi^2 E I_y}{L^2} \qquad\qquad P_x = \frac{\pi^2 E I_x}{L^2} \tag{28}$$

In a similar manner, the definitions for U_u and U_v can be stated in terms of x and y axis properties by substituting Eq. 20 into Eq. 3, which reduces to these straightforward transformations:

$$U_u = U_x \cos\alpha - U_y \sin\alpha \qquad\qquad U_v = U_y \cos\alpha + U_x \sin\alpha \tag{29}$$

where

$$U_x = \int y^3 dA + \int x^2 y dA \qquad\qquad U_y = \int x^3 dA + \int y^2 x dA \tag{30}$$

Then utilizing Eq. 20 for the shear center coordinates (x_o, y_o) in Eq. 2, and substituting the results into the expressions for β in Eq. 12 and Eq. 17, provides the following relationships:

$$\beta_y = \frac{U_u}{2I_u}\cos\alpha + \frac{U_v}{2I_v}\sin\alpha - y_o \qquad \beta_x = \frac{U_v}{2I_v}\cos\alpha - \frac{U_u}{2I_u}\sin\alpha - x_o \tag{31}$$

Further substitutions using Eq. 29 and the relationships in Eqs. 23 to 26 lead to these final forms in terms of x and y section properties:

$$\beta_y = \frac{U_x I_y - U_y I_{xy}}{2\left(I_x I_y - I_{xy}^2\right)} - y_o \qquad\qquad \beta_x = \frac{U_y I_x - U_x I_{xy}}{2\left(I_x I_y - I_{xy}^2\right)} - x_o \tag{32}$$

Specific Cases

Principal Axes

If the support directions align with the principal axes, $I_{xy} = 0$. This simplifies the general solution such that P_y and P_x may be used in place of P'_y and P'_x , and the properties β_y and β_x do not require transformation. The solution is reduced to the following:

$$M_x = P_y\left[-\beta_y \pm \sqrt{\beta_y^2 + r_o^2 P_t/P_y}\right] \quad M_y = P_x\left[-\beta_x \pm \sqrt{\beta_x^2 + r_o^2 P_t/P_x}\right] \tag{33}$$

$$\beta_y = \frac{U_x}{2I_x} - y_o \qquad \beta_x = \frac{U_y}{2I_y} - x_o \tag{34}$$

Point-Symmetric

For point-symmetric sections, the shear center coincides with the centroid (i.e., $x_o = 0$, $y_o = 0$). Furthermore, the properties U_x and U_y are equal to zero, thus β_y and β_x are also zero. The lateral-torsional buckling equations take the following simpler form:

$$M_x = \pm r_o\sqrt{P'_y P_t} \qquad M_y = \pm r_o\sqrt{P'_x P_t} \tag{35}$$

Symmetric About X Axis

For any section symmetric about the x axis, including doubly-symmetric sections, the properties I_{xy}, U_x, y_o, and β_y are all zero. Therefore the lateral-torsional buckling equation for bending about the x axis is simply:

$$M_x = \pm r_o\sqrt{P_y P_t} \tag{36}$$

Symmetric About Y Axis

For any section symmetric about the y axis, including doubly-symmetric sections, the properties I_{xy}, U_y, x_o, and β_x are all zero. Therefore the lateral-torsional buckling equation for bending about the y axis is simply:

$$M_y = \pm r_o\sqrt{P_x P_t} \tag{37}$$

Fully Braced in X Direction

If a member is fully braced in the x direction, P'_y approaches infinity and $1/P'_y$ becomes zero. The M_x^2 term in Eq. 11 drops out, thus reducing the solution to Eq. 38. There is only one root to the equation, so the sign of β_y dictates the sign of the torsional buckling moment. If β_y is very small, the member is not subject to torsional buckling.

$$M_x = r_o^2 P_t / 2\beta_y \tag{38}$$

Fully Braced in Y Direction

If a member is fully braced in the y direction, P'_x approaches infinity and $1/P'_x$ becomes zero. The M_y^2 term in Eq. 16 drops out, thus reducing the solution to Eq. 39. There is only one root to the equation, so the sign of β_x dictates the sign of the torsional buckling moment. If β_x is very small, the member is not subject to torsional buckling.

$$M_y = r_o^2 P_t / 2\beta_x \tag{39}$$

Stress Representation

The above lateral-torsional buckling moment equations were developed using axial compressive forces. These can be restated using compressive stresses, where axial stress $\sigma = P/A$.

$$\boxed{M_x = A\sigma'_{ey}\left[-\beta_y \pm \sqrt{\beta_y^2 + r_o^2\sigma_t/\sigma'_{ey}}\right] \qquad M_y = A\sigma'_{ex}\left[-\beta_x \pm \sqrt{\beta_x^2 + r_o^2\sigma_t/\sigma'_{ex}}\right]} \tag{40}$$

$$\sigma'_{ey} = \sigma_{ey}\left(1 - \frac{I_{xy}^2}{I_x I_y}\right) \qquad \sigma'_{ex} = \sigma_{ex}\left(1 - \frac{I_{xy}^2}{I_x I_y}\right) \tag{41}$$

$$\sigma_{ey} = \frac{\pi^2 E}{(L/r_y)^2} \qquad \sigma_{ex} = \frac{\pi^2 E}{(L/r_x)^2} \tag{42}$$

$$\sigma_t = \frac{1}{Ar_o^2}\left(GJ + \pi^2 E C_w / L^2\right) \tag{43}$$

Principal Axes

$$M_x = A\sigma_{ey}\left[-\beta_y \pm \sqrt{\beta_y^2 + r_o^2\sigma_t/\sigma_{ey}}\right] \qquad M_y = A\sigma_{ex}\left[-\beta_x \pm \sqrt{\beta_x^2 + r_o^2\sigma_t/\sigma_{ex}}\right] \tag{44}$$

Point-Symmetric

$$M_x = \pm A r_o\sqrt{\sigma'_{ey}\sigma_t} \qquad M_y = \pm A r_o\sqrt{\sigma'_{ex}\sigma_t} \tag{45}$$

Symmetric About X Axis

$$M_x = \pm A r_o \sqrt{\sigma_{ey}\sigma_t} \tag{46}$$

Symmetric About Y Axis

$$M_y = \pm A r_o \sqrt{\sigma_{ex}\sigma_t} \tag{47}$$

Fully Braced in X Direction

$$M_x = A r_o^2 \sigma_t / 2\beta_y \tag{48}$$

Fully Braced in Y Direction

$$M_y = A r_o^2 \sigma_t / 2\beta_x \tag{49}$$

Illustrative Example

Given the eave strut section shown in Figure 2 with the section properties provided in Table 1, determine the positive and negative lateral-torsional buckling moments about the *x* and *y* axes for various unbraced lengths.

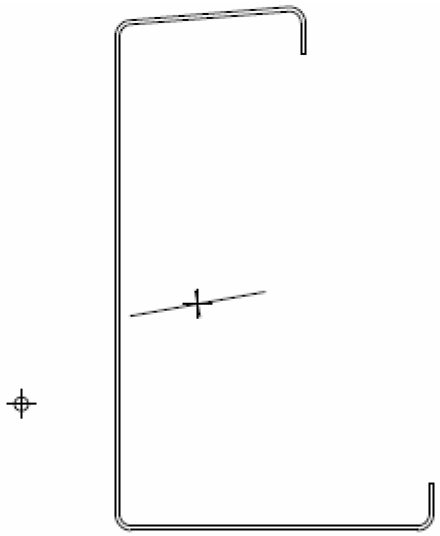

Figure 2. Eave Strut 8x5x3x14ga

Table 1: Section Properties for Eave Strut 8x5x3x14ga

A	1.162	in^2	I_{xy}	–1.754	in^4
I_x	12.317	in^4	I_y	2.873	in^4
U_x	5.035	in^5	U_y	9.637	in^5
r_x	3.256	in	r_y	1.572	in
x_o	–2.771	in	y_o	–1.574	in
I_o	26.991	in^4	r_o	4.820	in
J	0.001844	in^4	C_w	22.89	in^6

Calculate β_y and β_x using Eq. 32

$$\beta_y = \frac{(5.035)(2.873)-(9.637)(-1.754)}{2[(12.317)(2.873)-(-1.754)^2]} - (-1.574) = 2.059\ in$$

$$\beta_x = \frac{(9.637)(12.317)-(5.035)(-1.754)}{2[(12.317)(2.873)-(-1.754)^2]} - (-2.771) = 4.744\ in$$

Calculate positive M_x for L = 300 in

$$\sigma_t = \frac{1}{1.162(4.820)^2}[11300(0.001844) + \pi^2 29500(22.89)/300^2] = 3.515\ ksi$$

$$\sigma'_{ey} = \frac{\pi^2 29500}{(300/1.572)^2}\left[1 - \frac{(-1.754)^2}{(12.317)(2.873)}\right] = 7.299\ ksi$$

$$M_x = 1.162(7.299)\left[-2.059 + \sqrt{2.059^2 + 4.820^2(3.515/7.299)}\right] = 15.85\ k\text{-}in$$

Calculate positive M_y for L = 300 in

$$\sigma_t = \frac{1}{1.162(4.820)^2}[11300(0.001844) + \pi^2 29500(22.89)/300^2] = 3.515\ ksi$$

$$\sigma'_{ex} = \frac{\pi^2 29500}{(300/3.256)^2}\left[1 - \frac{(-1.754)^2}{(12.317)(2.873)}\right] = 31.31\ ksi$$

$$M_y = 1.162(31.31)\left[-4.744 + \sqrt{4.744^2 + 4.820^2(3.515/31.31)}\right] = 9.73\ k\text{-}in$$

Calculate negative M_x for L = 480 in

$$\sigma_t = \frac{1}{1.162(4.820)^2}[11300(0.001844) + \pi^2 29500(22.89)/480^2] = 1.843\ ksi$$

$$\sigma'_{ey} = \frac{\pi^2 29500}{(480/1.572)^2}\left[1 - \frac{(-1.754)^2}{(12.317)(2.873)}\right] = 2.851\ ksi$$

$$M_x = 1.162(2.851)\left[-2.059 - \sqrt{2.059^2 + 4.820^2(1.843/2.851)}\right] = -21.36\ k\text{-}in$$

Calculate negative M_y for L = 960 in

$$\sigma_t = \frac{1}{1.162(4.820)^2}[11300(0.001844) + \pi^2 29500(22.89)/960^2] = 1.040\ ksi$$

$$\sigma'_{ex} = \frac{\pi^2 29500}{(960/3.256)^2}\left[1 - \frac{(-1.754)^2}{(12.317)(2.873)}\right] = 3.058\ ksi$$

$$M_y = 1.162(3.058)\left[-4.744 - \sqrt{4.744^2 + 4.820^2(1.040/3.058)}\right] = -36.45\ k\text{-}in$$

Finite strip analyses for these cases produced the following results, which are within 0.5% of the calculated values: M_x = 15.85 *k-in*, M_y = 9.71 *k-in*, M_x = –21.34 *k-in*, M_y = –36.29 *k-in*.

Impact on Design

For singly-symmetric and doubly-symmetric sections, the AISI (2016) provisions are equivalent to Eqs. 44, 46, and 47. For point-symmetric sections, the AISI provisions apply a reduction factor of 0.5 to Eq. 46. However, this reduction factor should depend on the section geometry as reflected in Eq. 45. The ratio of Eq. 45 to Eq. 46 quantifies the reduction factor as $\sqrt{1 - I_{xy}^2/I_x I_y}$.

The AISI Design Manual (2013) contains several tables and charts for ordinary Zee sections. Table 2 below provides a comparison of the elastic buckling stress calculations for these sections, where one thickness was chosen to represent each size. The 0.5 reduction factor used in the current AISI provisions is very conservative for these sections, averaging 27% below the theoretical elastic buckling stress. The finite strip method (FSM) provided elastic buckling stresses which essentially match the theoretical values.

Table 2: Lateral-torsional buckling stress for various Zee shapes

Section (L = 180 in)	F_{cre} (ksi)	$F_{cre\ AISI}$ (ksi)	$F_{cre\ FSM}$ (ksi)	$F_{cre\ AISI}$ / F_{cre}	$F_{cre\ FSM}$ / F_{cre}
12ZS3.25x105	21.43	15.24	21.23	0.711	0.991
12ZS2.75x105	16.52	11.50	16.42	0.696	0.994
12ZS2.25x105	12.20	8.29	12.14	0.679	0.996
10ZS3.25x105	22.09	16.15	21.95	0.731	0.994
10ZS2.75x105	17.22	12.32	17.14	0.716	0.995
10ZS2.25x105	12.90	9.01	12.86	0.698	0.997
9ZS2.25x105	13.33	9.46	13.29	0.709	0.997
8ZS3.25x105	22.96	17.32	22.83	0.755	0.994
8ZS2.75x105	18.15	13.41	18.08	0.739	0.996
8ZS2.25x105	13.86	9.99	13.84	0.721	0.999
7ZS2.25x105	14.53	10.66	14.52	0.734	0.999
6ZS2.25x105	15.44	11.54	15.45	0.747	1.000
4ZS2.25x070	15.70	12.16	15.71	0.774	1.000
3.5ZS1.5x070	9.00	6.86	9.01	0.762	1.001
			Average	0.727	0.997
			Std Dev	0.027	0.003

The proportions of these Zee sections are similar, so the level of conservatism (22% to 32%) is fairly consistent. However, the product of inertia I_{xy} is sensitive to the web angle of a Zee section.

Figure 3 illustrates how changes to the web angle for the sections in Table 2 impact the ratio of the AISI buckling stress to the theoretical buckling stress, which varies by ±50%. For extreme cases where I_{xy}^2 approaches $I_x I_y$, the theoretical buckling stress approaches zero and the AISI provisions become very unconservative.

The AISI Specification provides an alternate, simpler equation, which is also plotted in Figure 3. For Zee sections with 90° webs, this equation provides acceptable, conservative results. For other web angles, the alternate equation is either very conservative or very unconservative.

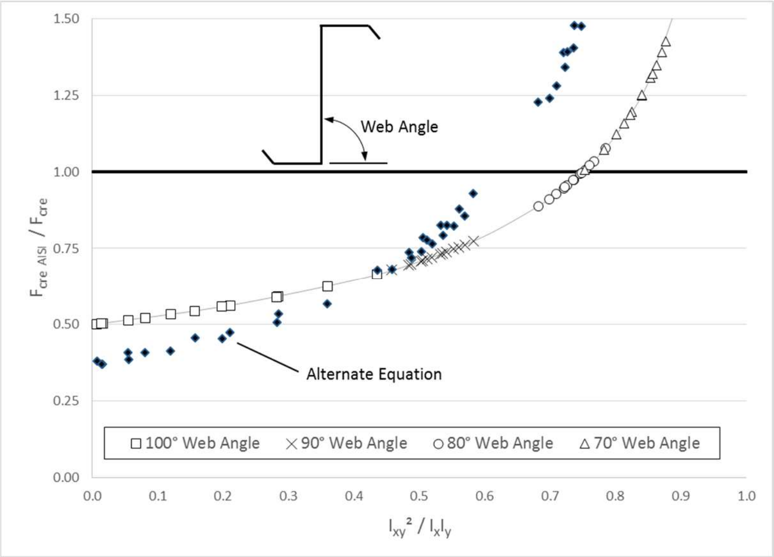

Figure 3. Comparison of AISI to theoretical elastic buckling stress for various Zee shapes

For angles and any other sections not oriented to the principal axes, there are no AISI provisions for lateral-torsional buckling, although numerical analyses such as the finite strip method may be applied as a rational analysis.

Conclusions

A general lateral-torsional buckling equation has been developed which is applicable to any cold-formed steel shape. Two factors in this equation were defined using principal axis properties of the cross-section, but axis transformations developed herein permit calculation of these factors using *x* and *y* axis section properties which correspond to the member orientation.

Buckling stress predictions were compared to numerical solutions for a variety of sections and lengths. The finite strip method provided very good agreement. Cases with large slenderness had extremely close results, whereas slight deviations were observed as slenderness decreased.

This development fulfills a specific need in the industry to accurately predict lateral-torsional buckling strength for point-symmetric and non-symmetric shapes. The current AISI provisions for point-symmetric sections were shown to be overly conservative for common Zee shapes. For some less common point-symmetric sections, the AISI provisions could be very unconservative. It is therefore recommended that the AISI provisions be modified to use this elastic buckling equation.

Currently AISI has no provisions for lateral-torsional buckling of non-symmetric shapes. The inclusion of this general buckling equation will benefit the engineer so that more complex rational methods such as finite strip analysis are not required.

Notation

A	Area of cross-section
C_w	Torsional warping constant
E	Modulus of elasticity
e_u, e_v	Eccentricity of axial load relative to u and v axes
e_x, e_y	Eccentricity of axial load relative to x and y axes
G	Shear modulus of elasticity
J	Saint-Venant torsion constant
I_u, I_v	Moment of inertia about principal u and v axes
I_x, I_y	Moment of inertia about x and y axes
I_{xy}	Product of inertia about x and y axes
L	Beam length
M_x, M_y	Critical elastic buckling moment about x and y axes
P	Critical elastic buckling axial load
P_u, P_v	Critical axial load for elastic buckling about principal u and v axes
P_x, P_y, P_t	Critical axial load for elastic buckling about x axis, y axis, and torsion
P'_x, P'_y	Adjusted axial load for elastic buckling about non-principal x and y axes
r_o	Polar radius of gyration about shear center
r_x, r_y	Radius of gyration about x and y axes
U_u, U_v	Geometric properties of cross-section as defined in Eq. 3
U_x, U_y	Geometric properties of cross-section as defined in Eq. 30
u, v	Principal coordinate axes of cross-section
u, v, ϕ	Buckling displacements in the u and v directions, and angle of twist
u'', v'', ϕ''	Second derivative of buckling displacements with respect to longitudinal axis
u'''', v'''', ϕ''''	Fourth derivative of buckling displacements with respect to longitudinal axis
u_o, v_o	Principal axis coordinates of shear center relative to centroid

x, y	Coordinate axes of cross-section corresponding to support directions
x_o, y_o	Coordinates of shear center relative to centroid
α	Angle of u principal axis measured counter-clockwise from x axis
β_u, β_v	Geometric properties of cross-section as defined in Eq. 2
β_x, β_y	Geometric properties of cross-section as defined in Eq. 32
σ_{ex}, σ_{ey}, σ_t	Critical axial stress for elastic buckling about x axis, y axis, and torsion
σ'_{ex}, σ'_{ey}	Adjusted axial stress for elastic buckling about non-principal x and y axes

References

American Iron and Steel Institute (2013), *Cold-Formed Steel Design Manual*, 2013 Edition, Washington, DC, 2014.

American Iron and Steel Institute (2016), *North American Specification for the Design of Cold-Formed Steel Structural Members*, 2016 Edition, Washington, DC, 2016.

Peköz, T.B. and Winter, G. (1969), "Torsional Flexural Buckling of Thin-Walled Sections under Eccentric Load," *Journal of the Structural Division*, ASCE, Vol. 95, No. ST5, May 1969.

Timoshenko, S.P. and Gere, J.M. (1961), *Theory of Elastic Stability*, 2nd Edition, McGraw-Hill, New York, NY, 1961.

Vlasov, V.Z. (1961), *Thin-Walled Elastic Beams*, National Science Foundation, Washington, D.C., 2nd Edition, 1961.